The Preparation of Ternary Nanocomposite $TiO_2/ZrO_2/SnO_2$ by Double Template and Application for Water Purification

[1]CHUNHUA LU*, [2]XIAOYU SUN, [3]JUN PENG AND [3]YUBO MA

[1]*Department of Applied Chemistry Engineering, Jilin Vocational College of Industry and Technology Jilin, 132013, P.R. China.*

[2]*China Environmental United (Beijing) Environment Protection co Ltd , Beijing 100013, China.*

[3]*Northeast Normal University, Changchun 130024 , China.*

luchunhua1000@126.com*

(Received on 30th July 2012, accepted in revised form 14th December 2012)

Summary: $TiO_2/ZrO_2/SnO_2$ nanocomposite with large pore is prepared by sol-gel method with Pluronic P123 and Macrogol 20000 as double template. The structure and physicochemical property of the composite are characterized by small-angle powder X-ray diffraction (SAXS), wide-angle powder X-ray diffraction (WA-XRD) and N_2 adsorption-desorption. The photocatalytic efficiencies of the product are assessed by monitoring the photodegradation of Rhodamine B (RhB).The results show that the doping of SnO_2 retard the crystal phase transformation from anatase-TiO_2 to rutile-TiO_2; the doping of ZrO_2 stabilizes the anatase phase, and the phase transformation can be greatly retarded; the materials have relatively regular pores and high specific surface area; two types of pores attributed to the usage of double template; the presence of SnO_2 significantly increase the degradation rate; the materials can be used five times without decreasing their photocatalytic capacities significantly.

Keywords: double template; sol-gel method; photocatalytic properties; Rhodamine B.

Introduction

The treatment of highly colored wastewater containing hazardous industrial chemical materials is of great interest and importance for environmental protection consideration in the present time. Rhodamine B (RhB), as an important representative of xanthene dyes, is famous for its good stability as dye material. It has been widely used as food additives, but now it is forbidden. It may cause progressive and irreversible damage to cells, lungs, liver and finally leading to cancer. Various physical and chemical techniques had been used for the removal of organics from wastewaters. Such as coagulation, adsorption, chemical oxidation and froth flotation processes [1-4]. Recently, many other methods like electrochemical, photochemical techniques, etc [5-6] was used for the removal from wastewaters among these methods, photocatalysis was an advanced oxidation process that could be used for the destruction of pollutants in a simple and efficient manner. It is one of the most economic and promising industrial effluent treatment processes.

Various photocatalysts had been studied in the process of photocatalysis. Such as $ZnWO_4$ [7], AgBr [8], ZnO [9], Bi_2WO_6 [10], $Ca(OH)_2$ [11] and so on . In these photocatalysts, the semiconductor photocatalysts have attracted great attention for their wide application in degradation of environmental pollutants [12, 13]. Among various semiconductor photocatalysts, titania has proven to be suitable for widespread environmental applications due to its strong non-toxicity, stability, and resistance to chemical and optical corrosion. Cao *et al* [14] report that with more anatase content in the titania, photocatalytic activities can be improved gradually. While the anatase- titania is unstable, it will transfer to rutile-titania after calcined at 650 ^oC [15]. In view of the stability of anatase-titania in higher temperature, it is desired to develop modified photocatalysts. Thus, the modified of TiO_2 photocatalysts have been tried. Recently, there are some reports on metal oxide semiconductors that are active for organic compound degradation under visible light irradiation. Many references had proposed that the doping of transition metal oxides into TiO_2 could be an efficient method to obtain a preferable photocatalyst, such as WO_3 [16], Ag_2O [17], ZrO_2 [18, 19] and so on. Liu *et al* [20] and Wang *et al* [21] had reported that the doping of SnO_2 could increase the photoactivity up to several times. On the basis of these studies, ternary nanocomposite $TiO_2/ZrO_2/SnO_2$ by double template were prepared in this research work. The anatase- titania phase of the material can exist in high temperature. After calcing at 900 ^oC, the transformition from anatase- titania to anatase- titania is not occoured , and two types of pores attributed to the usage of double template are observed. In order to explore the photocatalytic

*To whom all correspondence should be addressed.

activity of the samples, the degradation of Rhodamine B is investigated. The results indicate that the photodegradation rate of RhB is enhanced after the doping of SnO_2.

Results and Discussion

WA-XRD

The WA-XRD patterns of TiO_2/ZrO_2 calcined at different temperatures are shown in Fig. 1. The characteristic diffraction peaks show that the samples have formed anatase-phase (JCPDSNo.21-1272), and the intensity of anatase becomes much higher and sharper with the calcination temperature from 200 to 800 °C, indicating that particle size grow bigger and have higher crystallinity [22]. The transformation from the anatase-phase to the rutile-phase (JCPDSNo.21-1276) occurs at 900 °C. With the increase of temperature, the diffraction of the rutile-phase (R) becomes stronger and the anatase-phase (A) weaker. While the reference [15] has reported that the pure TiO_2 shows both anatase and rutile phases after calcined at 650 ^oC. It is obvious that the doping of ZrO_2 stabilizes the anatase phase, and the phase transformation can be greatly retarded. The reference [14] has indicated that with less rutile content in the catalysts, photocatalytic activities can be improved gradually.

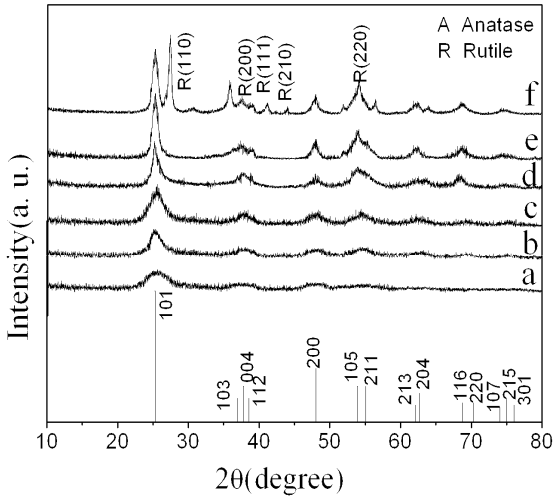

Fig. 1: WA-XRD patterns of TiO_2/ZrO_2 calcined at different temperatures.
(a TZ-200; b TZ-300; c TZ-500; d TZ-700; e TZ-800; f TZ-900;)

Fig. 2 shows WA-XRD patterns of $TiO_2/ZrO_2/SnO_2$ calcined at different temperatures. When the sample is calcined at 200 ^oC, the phase of the titania is amorphous. The anatase phase is observed at temperatures above 200^oC, and with the increase of temperature, the anatase phase is stronger and sharper, that indicates the enhancement of crystallization and the growth of crystallites. When the sample is calcined at 1000 ^oC, the phase transformation is detected, and no trace of diffraction peaks due to other phases like ZrO_2 or SnO_2 is observed. This shows that Zr^{4+} or Sn^{4+} may be dissolved in titania matrix [23] and hinders the phase transformation of titania from anatase to rutile markedly. The ionic radius of Zr^{4+} (0.079 nm) or Sn^{4+}(0.071 nm) is similar to that of Ti^{4+} (0.068 nm) [24, 25], so Zr^{4+} (0.079 nm) or Sn^{4+}(0.071 nm) ion moves into the titania matrix and substitutes it. This results in the delay of phase transformation of titania from anatase to rutile.

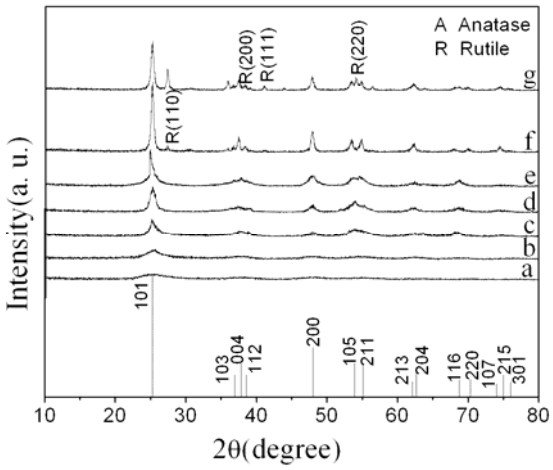

Fig. 2: WA-XRD patterns of $TiO_2/ZrO_2/SnO_2$ calcined at different temperatures.
(a TZS-200; b TZS-300; c TZS-500; d TZS-700; e TZS-800; f TZS-900; g TZS-1000;)

Small-Angle X-ray Scattering (SAXS)

Fig. 3 shows the SAXS patterns of TZ and TZS calcined at 800 ^oC. The intense diffraction peak can be indexed as the (100) reflection and the diffractions of (110) and (200) can not be detected. The presence of low angle reflections and absence of higher angle reflections suggests that while the pores may have uniform dimensions, the pore structure has relative low long range order [26, 27]. The result might be attributed to the compression of inorganic

matrix after the removal of template. When the SnO_2 is added (sample b), the diffraction peak of (100) shift to the low 2θ value, from 0.38° to 0.31°, indicating a probable thickening of the mesophase pore wall or a increasing of the pore diameter [28].

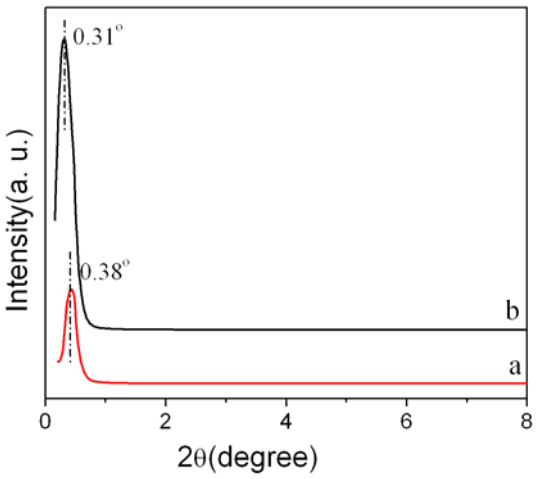

Fig. 3: SAXS patterns of TZ (a) and TZS(b) calcined at 800ºC.

N_2 Adsorption–Desorption

Nitrogen adsorption–desorption isotherm and the corresponding pore size distribution curve of TZ and TZS are shown in Fig. 4. The samples (Fig. 4 a) exhibit the type IV nitrogen isotherm, and the shape of the hysteresis loop is type H2 according to the IUPAC classification [29].A clear hysteresis loop is shown at a relative pressure between 0.4 and 0.7, related to the capillary condensation. This indicate that the samples have a large amount of mesopores [30], and the pores are ink-bottle-shaped or cage-type [31-32]. However, for sample TZS-800, at higher relative pressure between 0.8 and 0.95, the shape of the hysteresis loops is of the type H3 associated with aggregates of platelike particles that formed slitlike pores [33, 34].The pore size distribution curves (Fig. 4 b)implies that the materials have relatively regular pores. For each sample, there are two types of pores which are attributed to the usage of double template. These pores are mostly responsible for the specific surface area (Table-1) of the samples.

The specific surface area (S_{BET}), pore volume (V_p) and average pore diameter (d_P) of TZ and TZS calcined at 800 °C are presented in Table-1. The data in Table-1 show that the specific surface area, total pore volume and average pore diameter increase with the doping of SnO_2.The high specific surface areas are favorable for providing a suitable site for the high and uniform dispersion of active components. The results indicate that the doping of SnO_2 effectively inhibits grain growth of titania and delays the transformation of titania from anatase to rutile. The result is consistent with WA-XRD patterns.

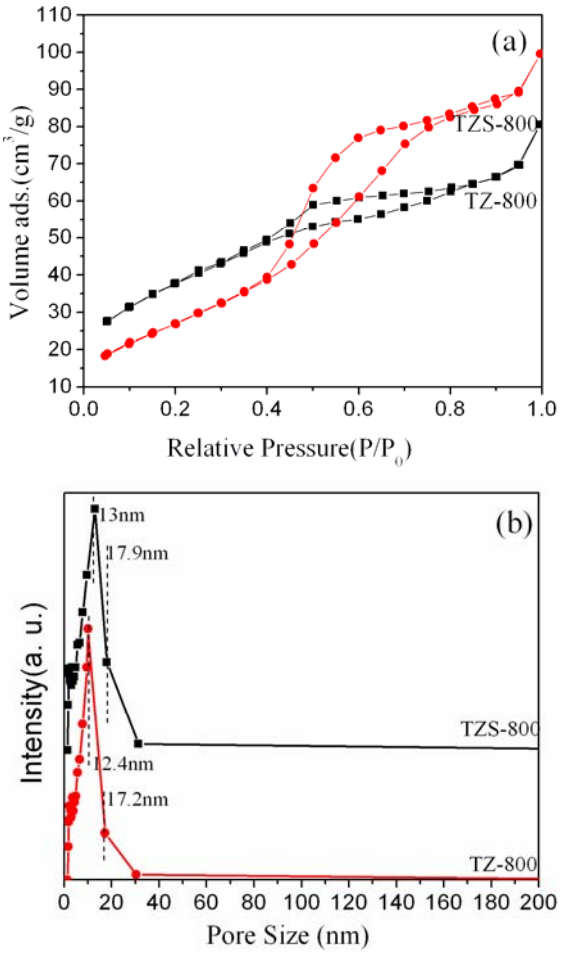

Fig. 4: Nitrogen adsorption–desorption isotherm (a) and the corresponding pore size distribution curve (b) of TZ and TZS.

Table-1: Textural and Structural Parameters of of TZ and TZS calcined at 800 °C.

Samples	d_P[a]/nm	S_{BET}[b]/m^2g^{-1}	V_p[c]/cm^3g^{-1}	phase
TZ-800	**12.4 and 17.2**	**136.9**	**0.107**	**anatase**
TZS-800	**13.0 and 17.9**	**159.9**	**0.171**	**anatase**

[a]The average pore diameter is estimated using the adsorption branch of the isotherm and Barret-Joyner-Halenda(BJH) model.
[b]The specific surface area is calculated by Brunauer-Emmett-Teller(BET)method.
[c]The total pore volume is taken from the adsorption branch of the nitrogen isotherm curve

SEM

Fig. 5 shows the SEM images of the TZS-800 before (a) and after waste treatment (b). It can be seen that the diameter of the sample before waste treatment is larger than that of after waste treatment. This indicates that the samples are split into small blocks in the process of the waste treatment, which can be attributed to the ultrasonic mixing.

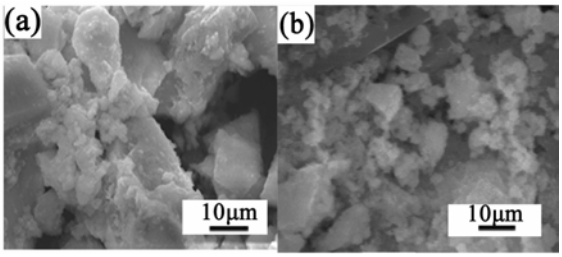

Fig. 5: SEM images of the TZS-800 before (a) and after waste treatment (b).

Photocatalytic Activity Tests

The photocatalytic properties of samples are evaluated by examination of RhB dye degradation. All the experiments are conducted at the neutral pH with a catalyst concentration of 0.2g. Under visible irradiation, the Rhodamine B is degraded with the color of the dispersion changing from an initial red color to a light green-yellow (Fig. 6). The photodegradations of Rhodamine B (initial concentration, 20 mg L^{-1}) under visible light irradiation (λ>420nm) by using TZ-800 (a) and TZS-800 (b) are depicted in Fig. 7. As seen in Fig. 7a, when the RhB solution is irradiated with visible light, the main absorbance (λ_{max}) that maximized at 555 nm can be observerd, and with the irradiation time, the wavelength of the major absorption band gradually shift to shorter wavelengths, from 555 nm to 498 nm (Fig. 7a inset), accompanied with the broadening of the absorption peaks. After 90 min of irradiation, the peak intensity further decreased to 0.0837. For sample TZS-800(Fig. 7b), with the irradiation time, the wavelength of the major absorption band gradually shift from 555 nm to 499 nm (Fig. 7b inset), and after 90 min of irradiation, the peak intensity completely diminished. This indicate that the doping of SnO_2 enhance the photocatalytic activity**.** The hypsochromic shift in λ_{max} of RhB is confirmed to be due to the step-by-step de-ethylation of RhB [35-37], and both the dye chromophores and the aromatic rings are destroyed; in other words, the RhB molecules are degraded instead of simply being decolorized [38-40].

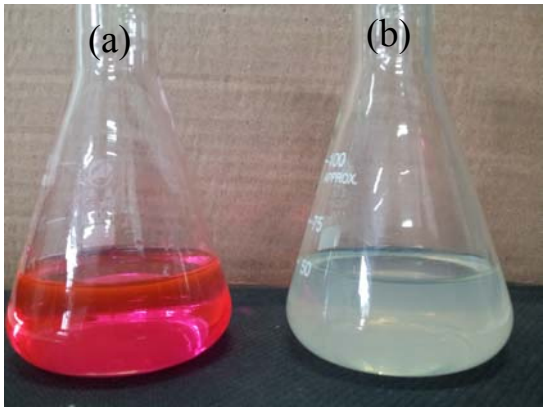

Fig. 6: The picture of the dye before (a) and after treatment (b).

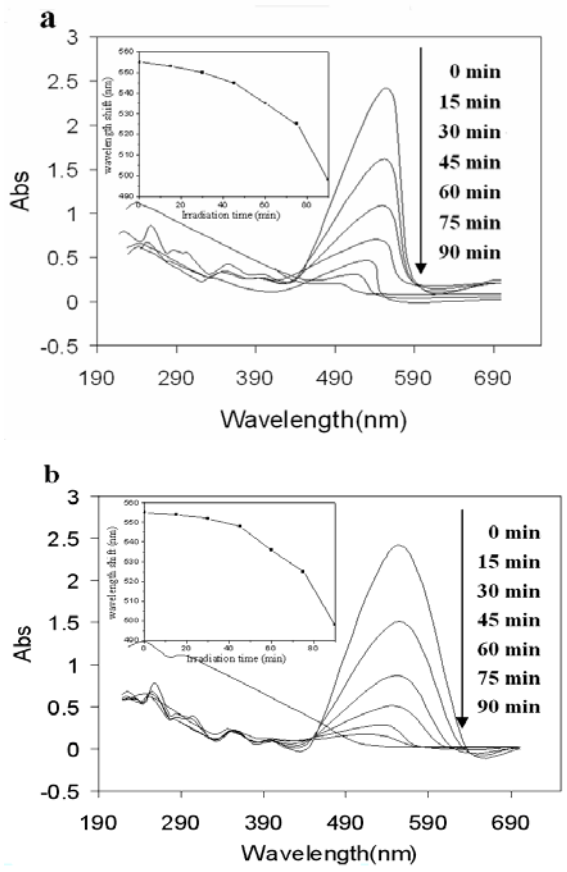

Fig. 7: The photodegradations of Rhodamine B (initial concentration, 20 mg L^{-1}) under visible light irradiation (λ>420nm) by using TZ-800 (a) and TZS-800 (b).

Fig. 8 shows photodegradation of RhB under different conditions. The y-axis of degradation was reported as C_i/C_0. C_i was the residual content of RhB after different irradiation time. C_0 was the original content of RhB. There was almost no degradation as the solution with TZS-800 in dark (Fig. 8a) and without any catalyst under visible light irradiation (Fig. 8b). It can be clearly seen that, minor removal of RhB occurs with catalyst TZ-800 unde UV irradiation (Fig. 8c). In the presence of TZS-800, the concentration of RhB decreased rapidly with irradiation time (Fig. 8d). An amount of 99.3% of RhB is removed using the TZS-800. While for TZ-800, only 91.2% of RhB is degraded after this illumination period. These results indicate that the addition of SnO_2 enhance the photodegradation of RhB.

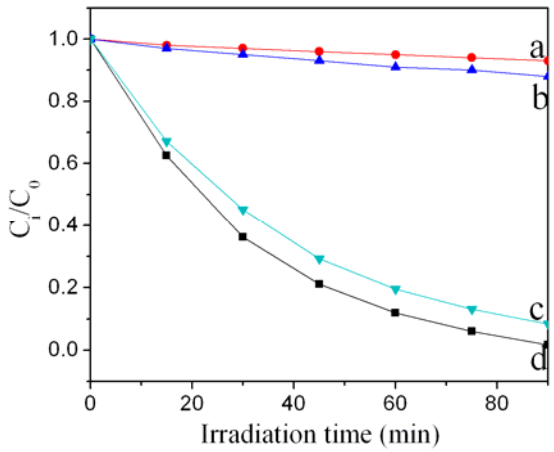

Fig. 8: Photodegradation of RhB under different conditions (a) with TZS-800 in dark, (b) without any catalyst and with visible light, (c) with TZ-800 (0.2 g) and visible light, (d) with TZS-800 (0.2 g) and visible light. (λ>420 nm; PH = 7; λ>420nm; initial concentration of RhB is 20 mg L^{-1}).

Fig. 9 shows concentration variation of RhB at various PHs of 5, 6, 7, 8 and 9, respectively. A variation in pH from 5 to 9 greatly influences the degradation of RhB. The photodegradation rate of the RhB dye decreased in turn at pH of 7, 6, 8, 5, 9, and a drastic decrease of the degradation rate is found at pH 7.

The regeneration of photocatalyst is one of key steps to make practical applications for the photocatalysis technology. An examination of the photocatalytic activity of the recycled film is carried out under UV light irradiation. The recyclability of the catalyst TZS-800 is shown in Fig. 10. It can be seen that the photocatalyst is recyclable for the removal of RhB under UV irradiation, although the photoactivity capacity gradually decreased from one cycle to another. The degradation rate is still higher and only decrease by 2% after 5 cycles.

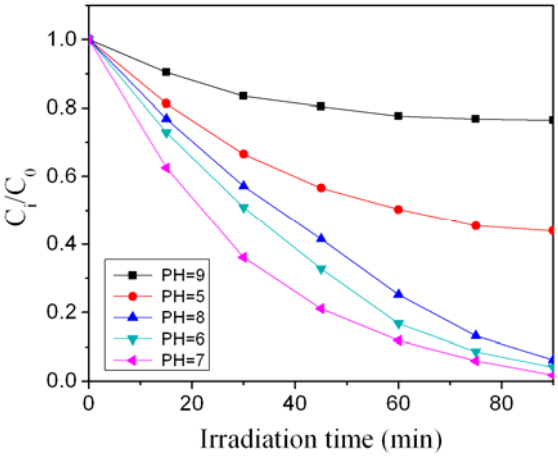

Fig. 9: The residual ratio (C_i/C_0) of RhB under different PHs. The amount of catalyst is 0.2 g ;λ>420nm; initial concentration of RhB is 20 mg L^{-1}.

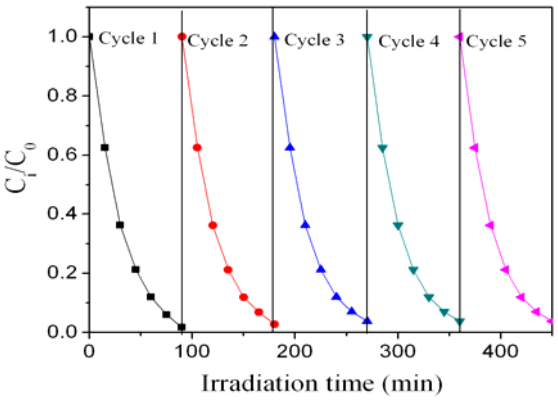

Fig. 10: Recycle of the TZS-800 for the degradation of RhB.

Experimental

Chemicals and Materials

Macrogol 20000 (PEG 20000) and Pluronic

P123 (M_w =5800) were purchased from Aldrich. Titanium butyrate (TBT), $ZrOCl_2 \cdot 8H_2O$ and $SnCl_4 \cdot 5H_2O$ were purchased from Tianjin Yongda Chemical Company. Nitric acid and ethanol were all purchased from Beijing Fine Chemical Company. Rhodamine B dye (*N*,*N*,*N*,*'N'*-tetraethylrhodamine, RhB) obtained from Junsei was of analytical reagent grade and used without further purification. The structure of RhB is shown below.

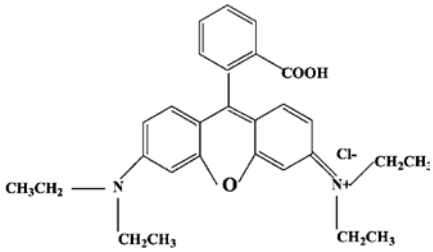

The structure of RhB

Synthesis

A typical sol-gel solution is prepared by adding ethanol (EtOH), Pluronic P123 (MW =5800) and Macrogol 20000 (PEG 20000) solutions to Titanium butyrate(TBT)/nitric acid mixed solutions under vigorous stirring at room temperature. The typical weights in grams of each component are TBT/ PEG/P123/ EtOH =6.8 g/8 g/2.3 g/100g. Subsequently the $ZrOCl_2 \cdot 8H_2O$ and $SnCl_4 \cdot 5H_2O$ are added drop wise with vigorous stirring at 80 °C until the mole ratio of Ti/Zr/Sn is 1:0.1:0.1. The obtained mixed solution is subsequently aged at room temperature for 24 h. The precipitate is recovered by filtration, washed with water repeatedly, and air-dried at room temperature. The template is removed by calcining for 5 h at different temperatures. Then the nanomaterial $TiO_2/ZrO_2/SnO_2$ is obtained, and designated as TZS-T (T is calcined temperature).

On the contrary, the manomaterial TiO_2/ZrO_2 are prepared by the same method. The samples are designated as TZ-T (T is calcined temperature).

Characterization

Powder X-ray diffraction (XRD) patterns are recorded on a Rigaku D/max-IIIB diffractometer using Cu Kα radiation (λ=1.5406 Å), and the amount of sample used for XRD is about 100mg. Nitrogen adsorption–desorption measurements (BET method) are performed at liquid nitrogen temperature, with an ASAP 2010 apparatus from Micromeritics. The analysis procedure is fully automated and operated with the static volumetric technique. Before each measurement, the samples are dehydrated first at 150 °C for 6 h and the amount is about 0.1g.

Photocatalytic tests

The photocatalytic activity of samples under irradiation of visible light is evaluated from an analysis of the photodegradation of Rhodamine B [41]. 0.2 g nanomaterial (TZ or TZS) is ultrasonically dispersed in 40 mL Rhodamine B solution (20 mg/L). After being stirred in dark for 30 min, the adsorption/desorption of Rhodamine B molecules on nanomaterial (TZ or TZS) reach equilibrium. The solution is then irradiated with a visible light (125W mercury lamp, a cut-off filter is used to remove the light with a wavelength below 400 nm). The concentration of solution is measured every 15min with a Cary 100 UV–visible spectrophotometer. The method of regeneration of photocatalyst is agreement with the reference [42].

Conclusion

$TiO_2/ZrO_2/SnO_2$ nanocomposite is prepared by sol-gel method with Pluronic P123 and Macrogol 20000 as double template. The results show that the doping of ZrO_2 and SnO_2 retard the crystal phase transformation from anatase-TiO_2 to rutile-TiO_2; the materials have relatively regular pores and high surface area; the presence of SnO_2 significantly increase the degradation rate; the materials can be used five times without decreasing their photocatalytic capacities significantly.

Acknowledgement

We gratefully acknowledge the financial support of this research by the National Natural Science Foundation (NSF) of China (No. 201110126) and Technology Planning Project from Education Department of JinlinProvince (No. [2012] 467)

References

1. B. D.Carlos, L. H. Ivonne, R. M. Gabriela, B. Bryan, and Patricia B.H. *Industrial and Engineering Chemistry Research*, **1253**, 48, (2009).

2. R. Katal, E.Hasani, M. Farnam, M. S.Baei and M. A.Ghayyem. *Journal of Chemical and Engineering Data*, **374**, 57 (2012).
3. P. B.Vijayalakshmi, G. Raju, A. Gnanamani. *Industrial and Engineering Chemistry Research*, **10194**, 50 (2011).
4. H. Katalambula, R. Gupta *Energy Fuels*, **3392**, 23 (2009).
5. B. Wang, X. Chang and H. Z.Ma. *Industrial and Engineering Chemistry Research*, **8478**, 47 (2008).
6. D. Mohan, K. P.Singh, G. Singh, K. Kumar *Industrial and Engineering Chemistry Research*, **3688**, 41 (2002).
7. X. Zhao and Y. Zhu, *Environmental Science and Technology*, **3367**, 40 (2006).
8. L. Kuai, B. Geng, X. Chen, Y. Zhao and Y. Luo, *Langmuir*, **18723**, 26 (2010).
9. J. Das and D. Khushalani *Journal of Physical Chemistry* C, **8114**, 114 (2010).
10. H. Fu, C. Pan, W. Yao and Y. Zhu *Journal of Physical Chemistry* B, **22432**, 109 (2005).
11. C. C. Hu and H. S.Teng, *Journal of Physical Chemistry* C, **20100**, 114 (2010).
12. T. Arai, M. Yanagida, Y. Konishi, Y. Iwasaki, H. Sugihara and K. Sayama *Journal of Physical Chemistry* C, **7574**, 111 (2007).
13. Z. Zou, J. Ye and H. Arakawa *Chemistry of Materials*, **1765**, 13 (2001).
14. Y. Q. Cao, H. J. Long, Y. M. Chen and Y. A. Cao, *Acta Physico-Chimica Sinica*, **1088**, 25 (2009).
15. S. Y. Chang, S. F. Chen and Y. C. Huang *Journal of Physical Chemistry* C, **1600**, 115 (2011).
16. K. Y. Song, M. K. Park, Y. T. Kwon, H. W. Lee, W. J.Chung and W. I. Lee *Chemistry of Materials*, **2349**, 13 (2001).
17. W. Zhou, H. Liu, J. Wang, D. Liu, G. Du and J. Cui, *ACS Applied Materials and Interfaces*, **2385**, 2 (2010).
18. S. Polisetti, P. A.Deshpande, G. Madras *Industrial and Engineering Chemistry Research*, **12915**, 50 (2011).
19. X. Wang, J. C. Yu, Y. Chen and L. Wu, X.Fu *Environmental Science and Technology*, **2369**, 40 (2006).
20. L. Xu, E. M. P.Steinmiller and S. E. Skrabalak, *Journal of Physical Chemistry* C, **871**, 116 (2012).
21. C. Wang, C. Shao, X. Zhang and Y. Liu *Inorganic Chemistry*, **7261**, 48 (2009).
22. H. Zhao, W. Fu, H. Yang, Y. Xu, W. Zhao, Y. Zhang, H. Chen, Q. Jing, X. Qi, J. Cao, X. Zhou and Y. Li *Applied Surface Science*, **8778**, 257 (2011).
23. P. Periyat, K. V. Baiju, P. Mukundan, P. K. Pillai and K. G. K. Warrier, *Applied Catalysis* A-*General*, **13** , 349 (2008).
24. N. Bao, Z. Wei, Z. Ma, F. Liu and G. Yin *Journal of Hazardous Materials*, **129**, 174 (2010).
25. P. Cheng, M. P. Zheng, Y. P. Jin, Q. Huang, M. Y. Gu, *Materials Letters*, **2989**, 57 (2003).
26. J. Fan, C. Z. Yu, J. Lei, Q.Zhang, T. C. Li and B. Tu *Journal of the American Chemical Society*, **10794**, 127 (2005).
27. T. Yu, H. Zhang, X. W. Yan, Z. X. Chen, X. D. Zou and P. Oleynikov *Journal of Physical Chemistry* B, **21467**, 110 (2006).
28. W. P. Guo, X. Li and X. S.Zhao *Microporous and Mesoporous Materials*, **285**, 93 (2006).
29. L. Cui, Y. Wang, M. Niu, G.. Chen and Y. Cheng, *Journal of Solid State Chemistry*, **2785**, 182 (2009).
30. K. Schrijnemakers and E. F. Vansant *Journal of Porous Materials*, **83**, 8 (2001).
31. M. Wark, J. Tschicrh and O. Bartels *Microporous and Mesoporous Materials*., **247**, 84(2005).
32. K.M.Coakley, Y.X.Liu, M.D.McGehee *Advanced Functional Materials*, **301**, 13(2003).
33. T.Y.Peng, A.Hasegawa, J.R.Qiu, K.Hirao *Chemistry of Materials*, **2011**, 15(2003).
34. J.Liu, Q.Sun, Y.Fu, J. Shen *Journal of Colloid and Interface Science*, **216**, 335(2009).
35. J.Pan, M.Huhne, H.Shen, L.Xiao, P.Born, W.Mader, S.Mathur *Journal of Physical Chemistry C*, **17265**, 115(2011).
36. Y.Cao, T.He, Y.Chen, Y. Cao *Journal of Physical Chemistry C* , **3627**, 114(2010).
37. H.Fu, C.Pan, W.Yao, Y.Zhu *Journal of Physical Chemistry B*, **22432**, 109(2005).
38. X.Li, J. Ye *Journal of Physical Chemistry C*, **13109**, 111(2007).
39. H. M.Sung-Suh, J. R.Choi, H. J. Hah, S. M. Koo and Y. C. Bae *Journal of Photochemistry and Photobiology* A-*Chemistry*, **37**, 163 (2004).
40. J. M. Wu and T. W. Zhang *Journal of Photochemistry and Photobiology* A-*Chemistry*, **171**, 162 (2004).
41. M. Asiltürk, F. Sayılkan, S. Erdemoglu, M. Akarsu, H. Sayılkan, M. Erdemoglu and E. Arpac, *Journal of Hazardous Materials*, **164**, B129 (2006).
42. F. Wang and K. Zhang *Journal of Molecular Catalysis* A*: Chemical*, **101**, 345 (2011)